Biochemical and Biophysical Research Communications 430 (2013) 218–224

Contents lists available at SciVerse ScienceDirect

Biochemical and Biophysical Research Communications

journal homepage: www.elsevier.com/locate/ybbrc

Rossmann-fold motifs can confer multiple functions to metabolic enzymes: RNA binding and ribonuclease activity of a UDP-glucose dehydrogenase

Ana Barbas [a,1], Alma Popescu [b], Carlos Frazão [a], Cecília M. Arraiano [a,*], Arsénio M. Fialho [b,*]

[a] Instituto de Tecnologia Química e Biológica/Universidade Nova de Lisboa, Oeiras, Portugal
[b] Institute for Biotechnology and Bioengineering (IBB), Instituto Superior Técnico, Lisbon, Portugal

ARTICLE INFO

Article history:
Received 17 October 2012
Available online 5 November 2012

Keywords:
UDP-glucose desidrogenase
RNA
Ribonuclease
Rossmann fold
Mitochondrial ribonucleases

ABSTRACT

Metabolic enzymes are usually characterized to have one specific function, and this is the case of UDP-glucose dehydrogenase that catalyzes the twofold NAD^+-dependent oxidation of UDP-glucose into UDP-glucuronic acid. We have determined that this enzyme is also capable of participating in other cellular processes. Here, we report that the bacterial UDP-glucose dehydrogenase (UgdG) from *Sphingomonas elodea* ATCC 31461, which provides UDP-glucuronic acid for the synthesis of the exopolysaccharide gellan, is not only able to bind RNA but also acts as a ribonuclease. The ribonucleolytic activity occurs independently of the presence of NAD^+ and the RNA binding site does not coincide with the NAD^+ binding region. We have also performed the kinetics of interaction between UgdG and RNA. Moreover, computer analysis reveals that the N- and C-terminal domains of UgdG share structural features with ancient mitochondrial ribonucleases named MAR. MARs are present in lower eukaryotic microorganisms, have a Rossmannoid-fold and belong to the isochorismatase superfamily. This observation reinforces that the Rossmann structural motifs found in NAD^+-dependent dehydrogenases can have a dual function working as a nucleotide cofactor binding domain and as a ribonuclease.

1. Introduction

UDP-glucose dehydrogenase (Ugd; EC 1.1.1.22) catalyzes the twofold NAD^+-dependent oxidation of UDP-glucose (UDP-Glc) into UDP-glucuronic acid (UDP-GlcA) [1]. This enzyme is essential in many processes in a wide variety of organisms. In bacteria, the activated precursor UDP-GlcA is the source of glucuronic acid for the biosynthesis of many exopolysaccharides and capsules [2,3]. In plants, Ugd plays a regulatory role in the carbon flux toward cell wall and glycoprotein biosynthesis [4]. In mammals, UDP-GlcA has three major functions: (1) is essential for the biosynthesis of glycosaminoglycans; (2) catalyzes the hepatic glucuronidation of toxins; (3) is necessary for the transport of hormones through conjugation [5].

Ugds consist of three domains, namely a N-terminus Rossmann-like domain, where NAD-binds, a central domain involved in dimerization and where the catalytic apparatus resides, and a second Rossmann-like domain at the C-terminus [6–8]. These enzymes belong to a family of sugar nucleotide-modifying enzymes that catalyze a net four-electron oxidation and serves as both alcohol dehydrogenase and aldehyde dehydrogenase [8]. Biochemical studies and crystal structures of Ugds have contributed to the understanding of their mechanism of action [9], revealing the catalytic residues that are necessary for the twofold oxidation [1,6,10].

It has been known that certain metabolic enzymes can play diverse roles in the cell, thus acting as multifunctional proteins [11,12]. Example of these include RNA-binding capabilities that were found in eukaryotic NAD-dependent dehydrogenases, such as the human glyceraldehyde-3-phosphate dehydrogenase (GAPDH) [13], the human lactate dehydrogenase [14], the yeast mitochondrial NAD^+-dependent isocitrate dehydrogenase [15] and the bovine glutamate dehydrogenase [16]. Interactions of GAPDH with RNA have also been reported both *in vitro* and *in vivo* [17]. In common, these proteins possess Rossmann fold like domains consisting of a β-sheet sandwiched by multiple α helices that are associated with binding of NAD(P) co-factors [18]. Taken together, these studies provide evidences that the Rossmann fold is capable of serving as a RNA interacting domain [19]. Despite this finding, the mechanism of RNA interaction remains unclear.

Here we report that UgdG, a bacterial UGD from the gellan producer strain *Sphingomonas elodea* ATCC 31461 [20,21], is able to bind RNA substrates and cleave them, acting as a ribonuclease. We also demonstrate that the ribonucleolytic activity is not

* Corresponding authors.
E-mail addresses: cecilia@itqb.unl.pt (C.M. Arraiano), afialho@ist.utl.pt (A.M. Fialho).
[1] Current address: Instituto de Biologia Experimental e Tecnológica, Oeiras, Portugal.

0006-291X/$ - see front matter © 2012 Elsevier Inc. All rights reserved.
http://dx.doi.org/10.1016/j.bbrc.2012.10.091

affected by the addition of NAD^+, proving that in UgdG two independent binding and catalytic regions can co-exist – one for NAD^+ and one for RNA. Finally, we show that there is a structural similarity between UgdG (N- and C-terminal domains) and mitochondrial associated ribonucleases from lower eukaryotic microorganisms.

2. Materials and methods

2.1. Bacterial strains, plasmids and growth conditions

Escherichia coli strains used were grown in Luria broth (LB) at 37 °C with orbital agitation. Plasmid vectors used were pSTBlue-1 (Novagen) and pWH844 [22]. The plasmid pUgdG carrying the *ugdG* gene preceded by a sequence coding for six histidines was used [20]. When required, the culture medium was supplemented with ampicillin (150 μg/ml).

2.2. Overexpression and purification of His6-UgdG in E. coli

The UgdG overexpression was obtained by induction of the *E. coli* BL21/pUgdG culture with 0.1 mM isopropyl β-D-thiogalactoside (IPTG), (OD_{640nm} 0.5), followed by 3 h of cultivation. Two hundred milliliters of the *E. coli* culture was harvested by centrifugation, washed with cold 0.9% (w/v) NaCl, and resuspended in 3 ml of cold start buffer (1 mM phosphate buffer [pH 7.4], 50 mM NaCl, and 10 mM imidazole). Cells extracts were obtained by sonication, followed by centrifugation (18,000×*g* for 1 h at 4 °C) and applied to a HisTrap column (GE Healthcare). After several washes with cold start buffer containing increasing imidazole concentrations, the His_6-UgdG was eluted with 200 mM imidazole. Imidazole was removed replacing the buffer with a PD10 desalting column (GE Healthcare) by a solution 100 mM Tris–HCl (pH 8.7), 5 mM dithiothreitol (DTT). UgdG migrated as a single polypeptide with a molecular mass of 48.5 kDa (47.2 kDa from the native, plus 1.3 kDa corresponding to the His_6 tag). The SDS–PAGE gel revealed that the purity of the protein is higher than 95% (Fig. 1).

2.3. In vitro transcription of RNAs

SL9A and malE-malF RNAs were obtained by *in vitro* transcription using the plasmids pSL9A [23,1] and pCH77 [24] as templates, respectively. The transcription reactions were performed using the Riboprobe kit (Promega), in a 20 μl volume, containing 20 μCi of [α-^{32}P]-dUTP (GE Healthcare). Radioactively labeled RNA transcripts were purified on a 8% PAA/7 M urea gel as described [25].

2.4. Electrophoretic mobility shift assay (EMSA)

EMSAs were performed with SL9A and malE-malF mRNA substrates [26]. Mixtures containing UgdG were incubated for 10 min at 37 °C and analyzed in a 5% non-denaturing polyacrylamide gel. Binding reactions were performed in 10 μl of volume containing 100 mM Tris–HCl pH 8.7, 10 mM $MgCl_2$, 2 mM DTT, 20 nM of malE-malF or SL9A substrate (10,000 counts per minute per reaction) and increasing concentration of enzyme. Mixtures were incubated for 10 min at 37 °C and analyzed in a 5% non-denaturing polyacrylamide gel. The RNA–protein complexes were detected by using the phosphorImager system from Molecular Dynamics.

2.5. Surface plasmon resonance analysis – BIACORE

On flow cell 1 of the SA streptavidin sensor chip no substrate was added (blank cell). On flow cell 2 a 5′ biotinylated 25-nt RNA oligomer (5′-CCCGACACCAACCACUAAAAAAAAA-3′) was added. The target RNA was captured on flow cell 2 by injecting 20 μl of a 500 nM solution of the target RNA in 1 M NaCl at a 10 μl/min flow rate. The assay was run at 4 °C in a buffer containing 20 mM Tris–HCl pH 8, 100 mM KCl, 1 mM DTT and 25 mM EDTA. The UgdG was injected over flow cells 1 and 2 for 2 min at concentrations of 10, 25, 50, 100, 250, 500, 1000, 2500 and 5000 nM using a flow rate of 20 μl/min. Bound protein was removed with a 60 s wash with 2 M NaCl. Rate and equilibrium constants were calculated using the BIA EVALUATION 3.0 software, according to the fitting model 1:1 Langmuir Binding. The free energy difference, ΔG°, was obtained according to the van't Hoff equation [27].

2.6. Activity assays

Ribonucleolytic activity was assayed using two substrates: a 30 nts oligoribonucleotide, and the mRNAs malE-malF. The reactions were carried out in a volume of 10 μl containing 30 nM of RNA substrate (10,000 counts per minute per reaction), 20 mM Tris–HCl pH 8, 100 mM KCl, 1 mM $MgCl_2$ and 1 mM DTT. Reactions were started by the addition of 60 μM the enzyme and incubated at 37 °C. Samples were withdrawn at the time points defined and the reaction was stopped by adding formamide-containing dye with 10 mM EDTA. Reaction products were resolved in a 20% polyacrylamide/7 M urea and analyzed by autoradiography. The ribonucleolytic activity of UgdG was also assayed with the mRNAs malE-malF. Cleavage assays were performed at 37 °C in 15 μl of cleavage buffer [100 mM Tris–HCl pH 8.7, 10 mM $MgCl_2$ and 2 mM DTT]. 50 nM of the RNA substrate were denatured for 10 min at 90 °C in the Tris component of the assay buffer and allowed to re-anneal at 37 °C for 20 min prior to the addition of the other buffer components. The reaction was initiated by the addition of 15 μM of UgdG. Samples were withdrawn at the time-points and quenched in 3 volumes of formamide-containing dye. Reaction products were incubated at 90 °C for 5 min and analyzed on a 6% (w/w) polyacrylamide/7 M urea gel and analyzed by autoradiography.

2.7. Structural analysis

VAST program was used to search for 3D homologs of UgdG, PDB entry 4a7p [21]. A comparison and 3D alignment of N-terminal (residues 1–199) and C-terminal (residues 308–438) UgdG domains together with the *Leishmania donovani* MAR1 structure [28] was produced using PDBeFold (SSM). The resulting superposition was further fine tuned with MODELLER using 1.75 Å as radius cut-off to define homologous Cαs, and led to a final fit of 82 Cαs with 2.0 Å RMSD. Program DSSP was used to assign secondary structure elements and programs Tops and EdiTops were used to produce secondary structure topology diagrams. Pymol program was used to produce proteins 3D structure cartoons and solvent accessible surfaces, mapped with their electrostatic potential distribution calculated using program APBS. The crystal packing analysis of *L. donovani* was performed with the server PISA.

3. Results and discussion

3.1. UgdG, an UDP-glucose dehydrogenase can bind RNA molecules

To verify if the UgdG from *S. elodea* ATCC 31461, interacts with RNA we performed electrophoretic mobility shift assays (EMSA) using the *in vitro* synthesized and radioactively labeled malE-malF [25] and SL9A mRNAs [24]. Both of them are small transcripts (375 nt and 83 nt, respectively) that contain one or more stem-loop structures with single stranded extensions at the 5′- and

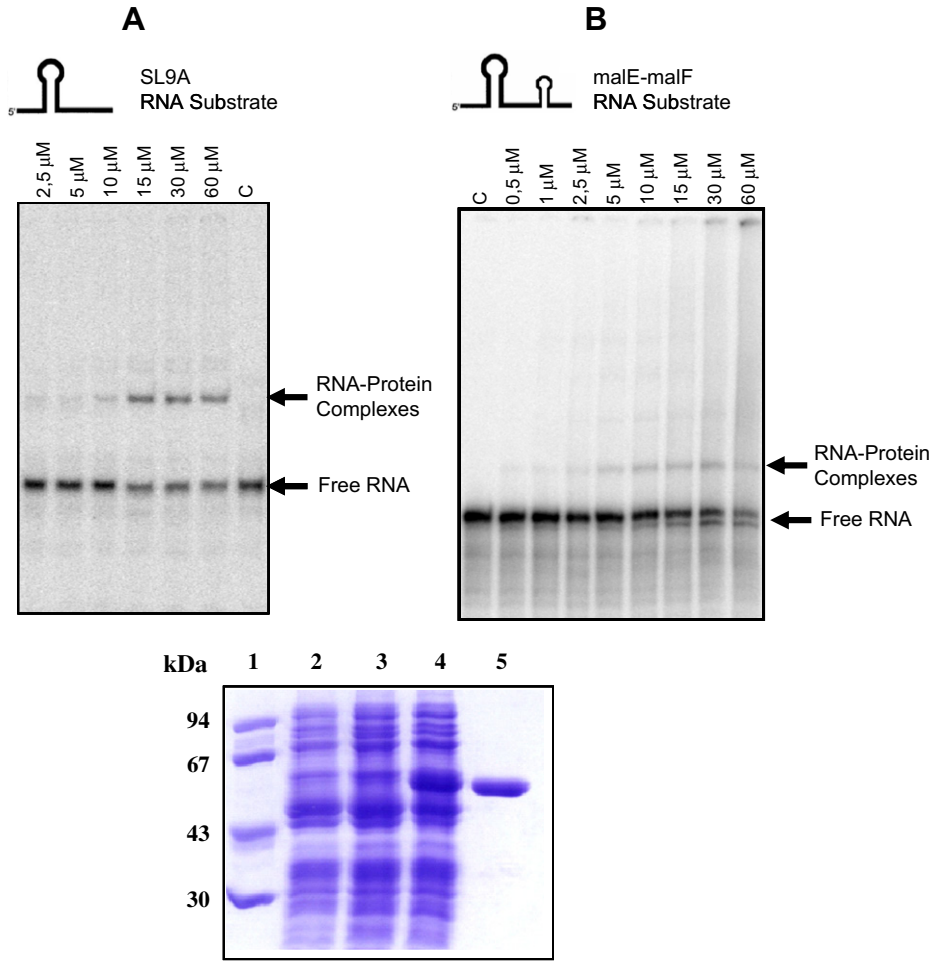

Fig. 1. Electrophoretic mobility shift assay of UgdG using mRNA transcript. 10,000 cpms of SL9A (A) or malE-malF (B) were incubated with UgdG. A control reaction and (c) without enzyme added was also performed. The bottom panel shows an SDS–PAGE gel prepared to guide the purification of His_6-UgdG overproduced in *E. coli* BL21cells. Lanes: 1, molecular marker; 2, soluble fraction from *E. coli* harboring the cloning vector pWH844; 3 and 4, soluble fractions from *E. coli* harboring the plasmid pUgdG harvested before and after IPTG induction; 5, fraction obtained by His-tag purification of UgdG.

3′-end of the molecule. Our results show that UgdG is able to bind to both substrates, generating retardation bands that correspond to RNA–protein complexes with 5 or 2.5 µM of protein for SL9A and malE-malF, respectively (Fig. 1). Previous reports have shown that other dehydrogenases (namely glyceraldehyde-3-phosphate dehydrogenase – GAPDH) exhibit RNA-binding ability [11,13]. Our results show that UDP-glucose dehydrogenase can also bind RNA.

3.2. In UgdG enzyme the RNA-binding site does not coincide with the NAD^+ binding region

Previous studies have established that the *in vitro* RNA binding ability of dehydrogenases was associated with the NAD-binding Rossmann-fold domain [13]. In an attempt to examine whether RNA and NAD^+ might compete for the same binding site on UgdG, we carried out competition assays. In an initial approach we performed an EMSA competition assay using malE-malF as a substrate and increasing concentrations of NAD^+. Two different concentrations of UgdG were used (10 and 30 µM), and the quantity of NAD^+ varied over the range of 0.25–3 mM. The range of NAD^+ concentrations used was based on previous studies that reported that the maximal UgdG dehydrogenase activity was found in the presence of 1 mM of NAD^+ [20]. Our results showed that the RNA–protein complexes were formed independently of the amount of NAD^+ present (Fig. 2). Our data suggests that in UgdG enzyme the

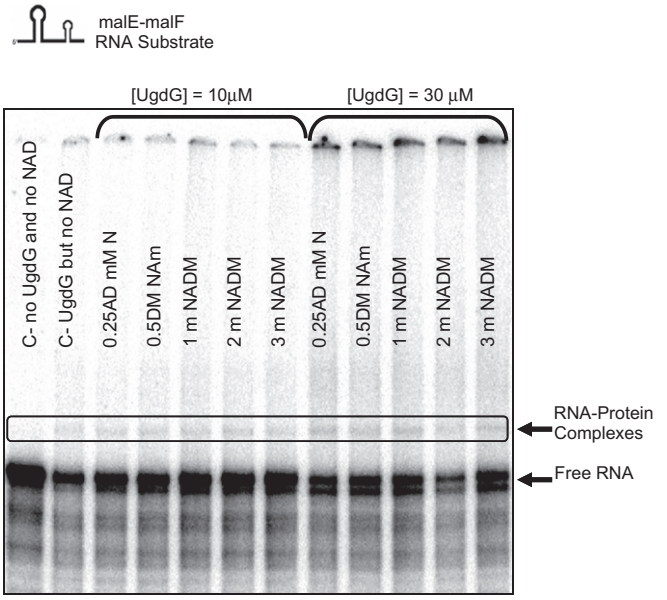

Fig. 2. Competition electrophoretic mobility shift assay of UgdG using mRNA transcript and NAD^+. 10,000 cpms of malE-malF were incubated with UgdG. Increasing amounts of NAD^+ were added to the reaction to analyze the competition between substrates.

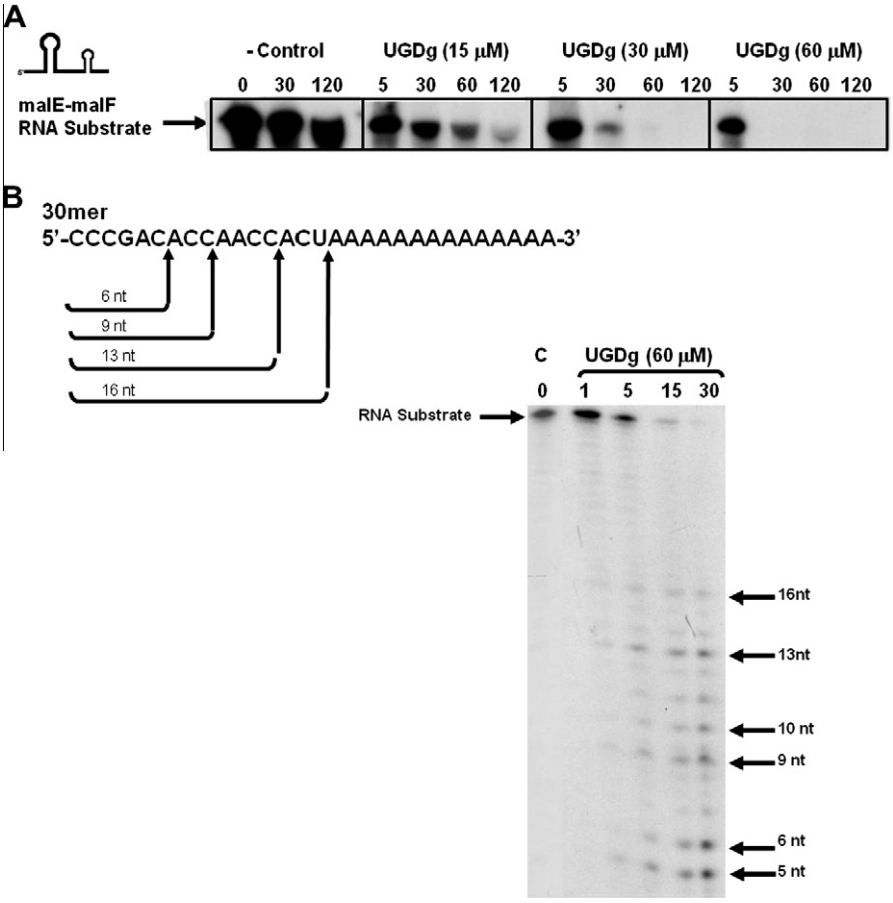

Fig. 3. Ribonucleolytic activity of UgdG using different RNA substrates. (A) The ribonucleolytic activity of UgdG was assayed with the *in vitro*-transcribed mRNAs malE-malF. Cleavage assays were performed with of 15, 30 and 60 μM of enzyme and samples were taken at the time-points indicated. Control reactions (c) were incubated during 0, 30 and 120 min with no enzyme added, and (B) activity assays were performed using the 30ss RNA substrate. Reactions were carried out with of 60 μM of enzyme.

binding regions for NAD^+ and RNA do not overlap. In accordance with our results, Evguenieva-Hackenberg et al. [17] reported that RNA binds to glyceraldehyde-3-phosphate dehydrogenase in a way that does not affect its ability to bind its common NAD^+ substrate. Contradictory data has however been reported concerning the binding sites of NAD^+ and RNA molecules within the Rossmann fold domain. Pioli et al. [14] proposed the existence of a coincident binding region for NAD^+ and RNA for the enzyme lactate dehydrogenase. Our studies reinforce the idea that in several dehydrogenases the RNA binding domain exerts its function independently of NAD^+.

3.3. Kinetic analysis of the interaction between UgdG and RNA

We have determined the kinetic constants for the interaction between UgdG and RNA (a 25 nt RNA oligomer) by Surface Plasmon Resonance (SPR). UgdG binds to RNA (K_d of 117 ± 11 nM), which is 18-fold higher than that reported for the prokaryotic exoribonuclease RNase II (6.5 ± 0.4 nM) [29], although in the same range. The dissociation constant measured is derived from a combination of both a rapid association [$k_a = (1.98 \pm 0.25) \times 10^5\ M^{-1}\ s^{-1}$] and a moderate dissociation [$k_d = (2.30 \pm 0.12) \times 10^{-3}\ s^{-1}$], confirming the ability of UgdG to form stable RNA complexes. Previous studies showed that *E. coli* wild-type RNase II has a fast association kinetics [$k_a = (3.3 \pm 0.3) \times 10^5\ M^{-1}\ s^{-1}$] and a slow dissociation kinetics [$k_d = (4.4 \pm 0.4) \times 10^{-4}\ s^{-1}$] [30] allowing the formation of RNA–protein complexes. Thus, comparing the kinetic analysis data from both UgdG and RNase II, it seems that these two proteins present a similar affinity for RNA. A thermodynamic analysis of RNA binding to UgdG enzyme based on van't Hoff equation was also performed. The result obtained for UgdG interaction with single-stranded RNA was $\Delta G = -36.78$ kJ/mol, while for *E. coli* RNase II this value ranges $\Delta G = -47.15$ kJ/mol [29]. In both cases the reaction is favorable and consequently the binding of RNA by UgdG is a spontaneous process.

3.4. UgdG exhibits ribonuclease activity

Since UgdG enzyme was binding RNA we investigated if it was able to degrade RNA. We used two mRNA transcripts (malE-malF and the 30mer single-stranded RNA substrates). In a set of assays we used the buffer for UgdG enzymatic activity towards its NAD^+ and UDP-glucose substrates – 100 mM Tris–HCl pH 8.7, 10 mM $MgCl_2$ and 2.5 mM DTT, and the reactions were carried out at 30 °C [20]. In another experiment, we assayed the ribonuclease activity using the buffer for *E. coli* ribonuclease II activity [31] – 20 mM Tris–HCl pH 8, 100 mM KCl, 1 mM $MgCl_2$ and 1 mM DTT, and the assays were done at 37 °C. Our results showed that when using the optimal reaction conditions for detection of ribonucleolytic activity in *E. coli* RNase II, we verified that UgdG is able to degrade the two mRNA substrates (data not shown). In the next step we assayed different concentrations of UgdG (15, 30 and 60 μM) using 50 nM of malE-malF mRNA. The ribonuclease activity assays revealed that UgdG degrades RNA similar to the activity of RNases (Fig. 3A). This relates to what was previously described

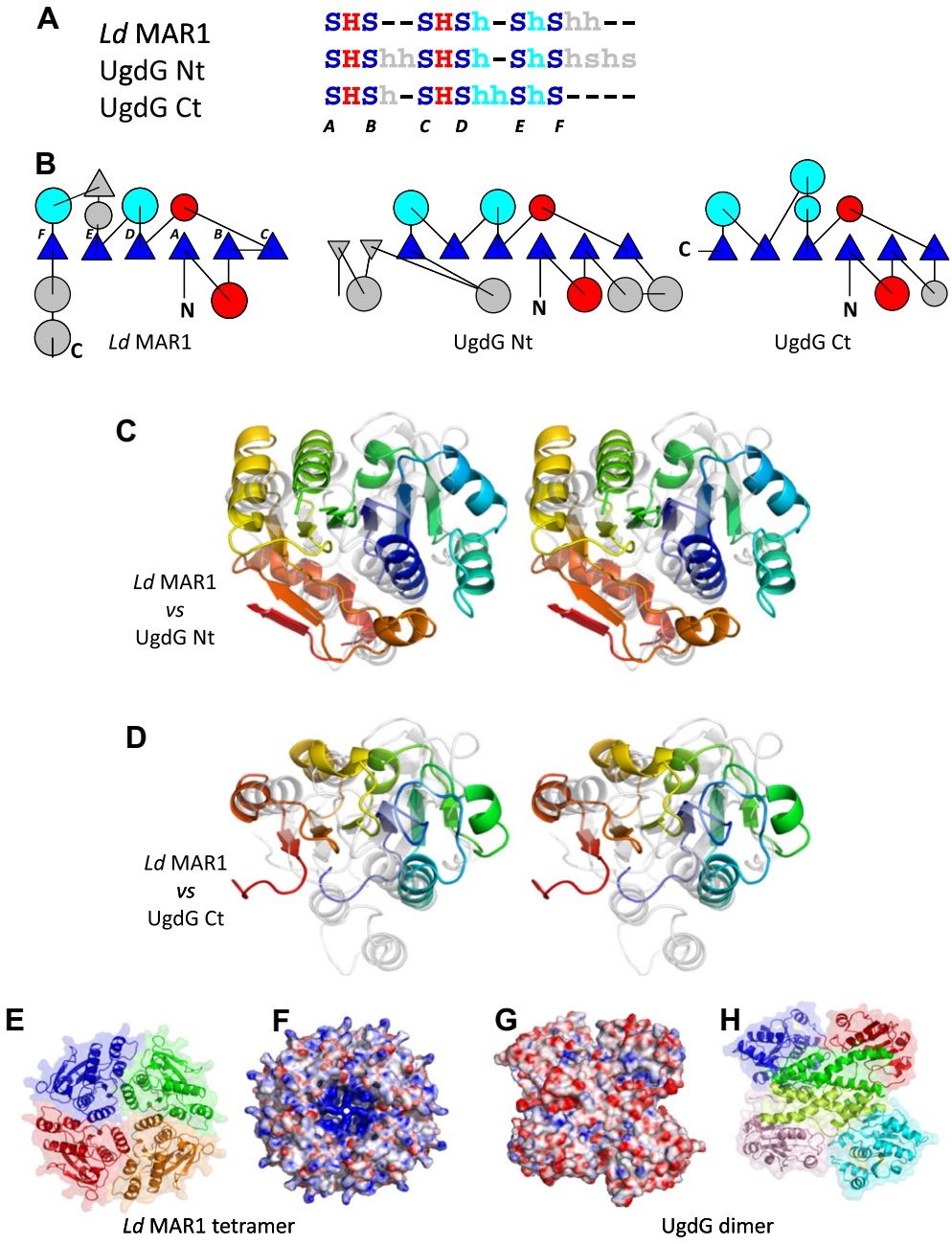

Fig. 4. Structural similarities between UgdG and mitochondrial ribonuclease (MAR1) from *L. donovani*. (A) Secondary structure matching between *L. donovani* MAR1 and the two Rossmann-like domains of UgdG ("s" – beta-strands, "h" – alpha-helices) with 3D superposition highlighted in upper-case. Blue and red correspond to conserved secondary structures, cyan to further homology correspondences and gray to unique features. (B) Topology diagrams of *L. donovani* MAR1, N- and C-terminal Rossmann-like domains of UgdG, showing beta-strands as triangles and alpha-helices as circles, color coded as in A. The Rossmann-fold internal beta-sheet shows its characteristic FEDABC strands arrangement. (C and D) Cartoons of *L. donovani* MAR1 (transparent gray) and (C) N-terminal and (D) C-terminal Rossmann-like domains of UgdG (colored blue to red from N- to C-termini) upon 3D superposition. (E–H) Views of (E and F) *L. donovani* MAR1 and (G and H) UgdG oligomers solvent accessible surfaces, mapped with (F and G) their electrostatic distributions or evidencing (E and H) their quaternary structures. The views show the central beta-sheet edge with carboxy end of the beta-strands, where nucleotides may bind. (For interpretation of the references to color in this figure legend, the reader is referred to the web version of this article.)

for glyceraldehydes-3-phosphate dehydrogenase but almost 100 times more protein was used in that assay (2 mM of protein and 20 nM of RNA transcript) [19]. When using 30 μM of enzyme there is a decrease in the RNA substrate along time, and after 60 min all the substrate has been consumed. When we increased the UgdG concentration to 60 μM the full length RNA substrate could no longer be detected after 30 min incubation. As such, we carried out assays using a different RNA substrate, a 30mer single-stranded RNA. UgdG seems to have preference for this substrate since it degraded it more efficiently, and after 15 min incubation with 60 μM enzyme more than half of the substrate had been cleaved. The analysis of the degradation products showed that there is accumulation of RNA fragments, ranging from 15 to 3 nt (Fig. 3B). Previous reports have shown that glyceraldehyde-3-phosphate dehydrogenase could cleave RNA between pyrimidine and adenine residues [17]. As such, by analyzing the sequence of the 30mer single-stranded RNA substrate we were able to hypothesize the same behavior for UgdG. The major generated RNA fragments seem to correspond to specific cleavage events that occur between C-A and U-A residues (Fig. 3B).

3.5. Structural similarities between UgdG and mitochondrial ribonucleases

Since we solved the UgdG structure (PDB entry 4a7p [21]) we searched databases for structural homologs. Beyond the similarities with Ugds, we observed a lower but discernible structural similarity with Mitochondrial Associated Ribonucleases (MAR) from lower eukaryotic microorganisms. Most notably, the 3D fit of *L. donovani* MAR1 structure [28] with N- and C-terminal Rossmann-like domains of UgdG led to superposition of 83 and 74 residues with 1.9 and 1.4 Å RMSDs, respectively. The 3D superposition corresponds to the alignment of the six *FEDABC* ordered beta-strands of the two consecutive motifs that build each Rossmann-like domain, as well as two of the interleaving helices (Fig. 4A–D). Although both terminal domains show the same topology, only that at the N-terminus includes the characteristic NAD binding motif GxGxxG, a loop between its first beta-strand and the following alpha-helix [32]. This motif provides main-chain interactions to the diphosphate, as found in the N-domain of the UgdG:NAD binary complex, PDB entry 4a7p. At the C-terminal domain the corresponding loop includes a 8 residues long insertion, after the glycine at the end of its first beta-strand, which occludes the otherwise putative NAD binding site. Furthermore, a comparison of MARs and Ugds quaternary structures shows further topological correspondences of their Rossmann-like domains 3D distribution (Fig. 4E–H, discussed below).

A search of annotated ribonucleases (MAR1) highlighted three crystal structures (1x9g, 1xn4 and 2b34), respectively from *L. donovani*, *L. major* and *Caenorhabditis elegans*. Furthermore, a fourth protozoan structure (1yzv) from *Trypanosoma cruzi* was found to be structurally closely related with those three, although annotated as a hypothetical protein. They can all be considered members of the isochorismatase superfamily [33]. Although there has been some controversy, they are classified as ribonucleases (MAR1) based on biochemical experimental evidences reported for a homologous protein from *Leishmania tarentolae* that has endoribonuclease activity [33].

Our analysis revealed that MAR1 molecules have in common a structural core that resembles a Rossmanoid fold (Fig. 4A and B). Moreover, their crystal packing analysis showed a common quaternary structure, always with four monomers localized around a (local) 4-fold rotational axis. Their contacts involve mainly their two C-terminal helices and occlude 20–28% of the otherwise solvent accessible area (Fig. 4E and F). Interestingly, Ugds are oligomeric structures as well with their helical middle subdomain also playing a crucial role in dimerization (Fig. 4H) [6]. Ugds dimers form sets of four Rossmann-like domains too being therefore reminiscent of MAR1 tetramers. However, while Ugds dimers only show 2-fold rotational symmetry, relating both N- and C-terminal Rossmann-like domains, in MAR1 the four monomers have their central beta-sheet arranged in a propeller-like architecture (Fig. 4E).

Although previous investigations have documented the ribonucleolytic activity of a few dehydrogenases [12], this is the first study that identifies structural similarity between the N- and C-terminal Rossmann-like domains of an Ugd and an exquisite group of mitochondrial ribonucleases named MAR [29]. These enzymes seem to be restricted to lower eukaryotic organisms and may represent the prototype of an ancient ribonuclease consisting of a Rossmannoid fold [19,28]. It is thus interesting to note that this observation is in accordance with published phylogenetic studies reporting the occurrence of Rossmann-like domains as an ancient RNA catalyst in the early evolution of life [19].

Altogether, our findings suggest that both the N- and the C-terminal Rossmann-like domains of UgdG are responsible for RNA binding and cleavage and the results can be extrapolated for the comprehension of the evolution of dehydrogenases. Furthermore, the dual activity of metabolic enzymes is certainly relevant for the understanding of the regulation of cell metabolism, allowing a complex and highly integrated interplay among different metabolic pathways.

Acknowledgments

AB and AP were recipients of Postdoctoral and doctoral fellowships funded by Fundação para a Ciência e a Tecnologia, Portugal (FCT), respectively. The work at ITQB was financed by grants from FCT (Pest-OE/EQB/LA0004/2001 and PTDC/QUI/67925/2006). IBB was financed through grants PTDC/BIA-MIC/71453/2006, PTDC/QUI/67925/2006 and PTDC/BIA-MIC/118386/2010.

References

[1] R.E. Campbell, S.C. Mosimann, I. van De Rijn, et al., The first structure of UDP-glucose dehydrogenase reveals the catalytic residues necessary for the two-fold oxidation, Biochemistry 39 (2000) 7012–7023.
[2] M.C. Laus, T.J. Logman, A.A. Van Brussel, et al., Involvement of exo5 in production of surface polysaccharides in *Rhizobium leguminosarum* and its role in nodulation of *Vicia sativa* subsp. *nigra*, J. Bacteriol. 186 (2004) 6617–6625.
[3] L. Wang, S. Li, Y. Li, Isolation and sequencing of glycosyltransferase gene and UDP-glucose dehydrogenase gene that are located on a gene cluster involved in a new exopolysaccharide biosynthesis in Streptomyces, DNA Sequence 14 (2003) 141–145.
[4] M. Klinghammer, R. Tenhaken, Genome-wide analysis of the UDP-glucose dehydrogenase gene family in *Arabidopsis*, a key enzyme for matrix polysaccharides in cell walls, J. Exp. Bot. 58 (2007) 3609–3621.
[5] S. Egger, A. Chaikuad, K.L. Kavanagh, et al., UDP-glucose dehydrogenase: structure and function of a potential drug target, Biochem. Soc. Trans. 38 (2010) 1378–1385.
[6] J. Rocha, A.O. Popescu, P. Borges, et al., Structure of *Burkholderia cepacia* UDP-glucose dehydrogenase (UGD) BceC and role of Tyr10 in final hydrolysis of UGD thioester intermediate, J. Bacteriol. 193 (2011) 3978–3987.
[7] V. Rajakannan, H.S. Lee, S.H. Chong, et al., Structural basis of cooperativity in human UDP-glucose dehydrogenase, PLoS One 6 (2011) e25226.
[8] X. Ge, L.C. Penney, I. van de Rijn, M.E. Tanner, Active site residues and mechanism of UDP-glucose dehydrogenase, Eur. J. Biochem. 271 (2004) 14–22.
[9] D. Feingold, J. Franzen, Pyridine nucleotide-linked four-electron transfer dehydrogenases, Trends Biochem. Sci. 6 (1981) 103–105.
[10] S. Egger, A. Chaikuad, M. Klimacek, et al., Structural and kinetic evidence that catalytic reaction of human UDP-glucose 6-dehydrogenase involves covalent thiohemiacetal and thioester enzyme intermediates, J. Biol. Chem. 287 (2012) 2119–2129.
[11] J.W. Kim, C.V. Dang, Multifaceted roles of glycolytic enzymes, Trends Biochem. Sci. 30 (2005) 142–150.
[12] J. Ciesla, Metabolic enzymes that bind RNA: yet another level of cellular regulatory network?, Acta Biochim Pol. 53 (2006) 11–32.
[13] E. Nagy, T. Henics, M. Eckert, et al., Identification of the NAD(+)-binding fold of glyceraldehyde-3-phosphate dehydrogenase as a novel RNA-binding domain, Biochem. Biophys. Res. Commun. 275 (2000) 253–260.
[14] P.A. Pioli, B.J. Hamilton, J.E. Connolly, et al., Lactate dehydrogenase is an AU-rich element-binding protein that directly interacts with AUF1, J. Biol. Chem. 277 (2002) 35738–35745.
[15] S.L. Anderson, V. Schirf, L. McAlister-Henn, Effect of AMP on mRNA binding by yeast NAD+-specific isocitrate dehydrogenase, Biochemistry 41 (2002) 7065–7073.
[16] T. Preiss, A.G. Hall, R.N. Lightowlers, Identification of bovine glutamate dehydrogenase as an RNA-binding protein, J. Biol. Chem. 268 (1993) 24523–24526.
[17] E. Evguenieva-Hackenberg, E. Schiltz, G. Klug, Dehydrogenases from all three domains of life cleave RNA, J. Biol. Chem. 277 (2002) 46145–46150.
[18] M. Gerstein, A structural census of genomes: comparing bacterial, eukaryotic, and archaeal genomes in terms of protein structure, J. Mol. Biol. 274 (1997) 562–576.
[19] F.J. Sun, G. Caetano-Anolles, The ancient history of the structure of ribonuclease P and the early origins of Archaea, BMC Bioinformatics 11 (2010) 153.
[20] A.T. Granja, A. Popescu, A.R. Marques, et al., Biochemical characterization and phylogenetic analysis of UDP-glucose dehydrogenase from the gellan gum producer *Sphingomonas elodea* ATCC 31461, Appl. Microbiol. Biotechnol. 76 (2007) 1319–1327.
[21] J. Rocha, A.T. Granja, I. Sa-Correia, et al., Cloning, expression, purification, crystallization and preliminary crystallographic studies of UgdG, an UDP-glucose dehydrogenase from *Sphingomonas elodea* ATCC 31461, Acta Crystallogr., Sect. F: Struct. Biol. Cryst. Commun. 66 (2007) 69–72.
[22] F. Schirmer, S. Ehrt, W. Hillen, Expression, inducer spectrum, domain structure, and function of MopR, the regulator of phenol degradation in *Acinetobacter calcoaceticus* NCIB8250, J. Bacteriol. 179 (1997) 1329–1336.

[23] C. Spickler, G.A. Mackie, Action of RNase II and polynucleotide phosphorylase against RNAs containing stem-loops of defined structure, J. Bacteriol. 182 (2000) 2422–2427.
[24] R.S. McLaren, S.F. Newbury, G.S. Dance, et al., MRNA degradation by processive 3′–5′ exoribonucleases in vitro and the implications for prokaryotic mRNA decay in vivo, J. Mol. Biol. 221 (1991) 81–95.
[25] C. Conrad, R. Rauhut, G. Klug, Different cleavage specificities of RNases III from *Rhodobacter capsulatus* and *Escherichia coli*, Nucleic Acids Res. 26 (1998) 4446–4453.
[26] M. Amblar, C.M. Arraiano, A single mutation in *Escherichia coli* ribonuclease II inactivates the enzyme without affecting RNA binding, FEBS J. 272 (2005) 363–374.
[27] P. Atkins, J. De Paula, Physical Chemistry, W.H. Freeman and Company, New York, NY, USA, 2006.
[28] J. Caruthers, F. Zucker, E. Worthey, et al., Crystal structures and proposed structural/functional classification of three protozoan proteins from the isochorismatase superfamily, Protein Sci. 14 (2005) 2887–2894.
[29] A. Barbas, R.G. Matos, M. Amblar, et al., Determination of key residues for catalysis and RNA cleavage specificity: one mutation turns RNase II into a "SUPER-ENZYME", J. Biol. Chem. 284 (2009) 20486–20498.
[30] R.G. Matos, A. Barbas, C.M. Arraiano, Comparison of EMSA and SPR for the characterization of RNA–RNase II complexes, Protein J. 29 (2010) 394–397.
[31] C.M. Arraiano, R.G. Matos, A. Barbas, RNase II: the finer details of the Modus operandi of a molecular killer, RNA Biol. 7 (2010) 276–281.
[32] C.R. Bellamacina, The nicotinamide dinucleotide binding motif: a comparison of nucleotide binding proteins, FASEB J. 10 (1996) 1257–1269.
[33] J.D. Alfonzo, O.H. Thiemann, L. Simpson, Purification and characterization of MAR1. A mitochondrial associated ribonuclease from *Leishmania tarentolae*, J. Biol. Chem. 273 (1998) 30003–30011.